Available online at www.sciencedirect.com
SCIENCE DIRECT
International Journal of Mass Spectrometry 252 (2006) 26–37
International Journal of Mass Spectrometry
www.elsevier.com/locate/ijms

On-road measurements of volatile organic compounds in the Mexico City metropolitan area using proton transfer reaction mass spectrometry

T.M. Rogers [a], E.P. Grimsrud [a,1], S.C. Herndon [b], J.T. Jayne [b], C.E. Kolb [b], E. Allwine [c], H. Westberg [c], B.K. Lamb [c], M. Zavala [d], L.T. Molina [d], M.J. Molina [d], W.B. Knighton [a,*]

[a] *Department of Chemistry and Biochemistry, Montana State University-Bozeman, Bozeman, MT 59717-3400, United States*
[b] *Aerodyne Research Inc., 45 Manning Road, Billerica, MA 01821-3976, United States*
[c] *Laboratory for Atmospheric Research, Department of Civil and Environmental Engineering, Washington State University, Pullman, WA 99164-2910, United States*
[d] *Department of Earth, Atmospheric and Planetary Sciences, Massachusetts Institute of Technology, Cambridge, MA 02139-4307, United States*

Received 8 December 2005; received in revised form 17 January 2006; accepted 17 January 2006
Available online 23 February 2006

Abstract

A proton transfer reaction mass spectrometer (PTR-MS) was redesigned and deployed to monitor selected hydrocarbon emissions from in-use vehicles as part of the Mexico City Metropolitan Area (MCMA) 2003 field campaign. This modified PTR-MS instrument provides the necessary time response (<2 s total cycle time) and sensitivity to monitor the rapidly changing hydrocarbon concentrations, within intercepted dilute exhaust emission plumes. Selected hydrocarbons including methanol, acetaldehyde, acetone, methyl tertiary butyl ether (MTBE), benzene and toluene were among the vehicle exhaust emission components monitored. A comparison with samples collected in canisters and analyzed by gas chromatography provides validation to the interpretation of the ion assignments and the concentrations derived using the PTR-MS. The simultaneous detection of multiple hydrocarbons in dilute vehicle exhaust plumes provides a valuable tool to study the impact of driving behavior on the exhaust gas emissions.

Keywords: PTR-MS; Proton transfer; Chemical ionization; Vehicle exhaust; VOC emissions

1. Introduction

The Mexico City Metropolitan Area (MCMA) has the reputation of having one of the worst air pollution problems in the world [1]. While policy initiatives enacted in the 1990s have led to significant improvements in certain emissions, the residents of this urban area are still significantly impacted by degraded air quality [1]. In the spring of 2003 an intensive 5-week field campaign was conducted to obtain a better understanding of the air quality problems in the MCMA megacity environment. A significant source of the air pollution in the MCMA arises from the nearly 3-million motorized vehicles operating in the area [2]. Vehicle exhaust contributes to the degradation of the air quality in urban environments due, in part, to the volatile organic component of these emissions, which contributes to the formation of ozone and secondary aerosol particles [3]. A considerable portion of the field campaign was aimed at the study and characterization of vehicle exhaust emissions of vehicles operated under real-world driving conditions. A mobile laboratory housing a combination of high time–response instruments with sufficient sensitivity to characterize diluted exhaust plumes was deployed. As part of the mobile laboratory a modified version of a commercial proton transfer reaction mass spectrometer (PTR-MS) was deployed for the first time for the measurement of selected volatile organic compounds (VOCs) in vehicle exhaust using the mobile laboratory as a chase vehicle [4,5].

* Corresponding author. Tel.: +1 406 994 5419; fax: +1 406 994 5407.
E-mail address: bknighton@chemistry.montana.edu (W.B. Knighton).
[1] Present address: Columbia Basin College, Pasco, WA, United States.

1387-3806/$ – see front matter © 2006 Elsevier B.V. All rights reserved.
doi:10.1016/j.ijms.2006.01.027

The PTR-MS with its sensitive rapid real-time measurement capability of selected VOCs in complex matrices makes the technique ideally suited for monitoring selected hydrocarbon emissions from on-road vehicles. The PTR-MS technique relies on the ionization of organic compounds in the gas phase through their reaction with H_3O^+ and the resulting ions are detected by mass spectrometry [6]. The technique allows for analysis of whole air samples without dilution, since the major components of air have proton affinities less than that of water and are not ionized. Except for the small alkanes, most organic compounds have proton affinities greater than that of water [7] and are ionized and detected using this technique. While proton transfer is considered to be a "soft" ionization technique forming predominately MH^+ (where M is the neutral organic molecule), ion mass alone is not a unique indicator of the neutral precursor. Fragmentation and secondary ion molecule reactions can further complicate the interpretation of the resulting mass spectrum. In this study, we monitored eight selected ions while driving on the roadways of the MCMA in 2003. These ions were chosen as monitors of the presence of methanol, acetaldehyde, methyl tertiary butyl ether (MTBE), acetone, benzene, toluene, C_8H_{10} (C2-benzenes) and C_9H_{12} (C3-benzenes) in the roadway airshed. The validity of these ion assignments is discussed in detail. Where overlap exists between the compounds being measured, the PTR-MS results are compared with gas chromatography flame ionization detection (GC-FID) analyses of air samples collected using a collocated whole air canister sampling system.

Specific case examples of hydrocarbon exhaust emission measurements made by the PTR-MS from different engine types are highlighted and include gasoline vehicles, with and without exhaust treatment systems, as well as a diesel vehicle. This limited set of examples is provided to demonstrate that the PTR-MS is a valuable analytical technique for real-time, in situ measurement of selected hydrocarbon engine exhaust emission products from in-use motor vehicles. A complete analysis of the motor vehicle exhaust emissions measured using the PTR-MS and other instruments on-board the Aerodyne mobile laboratory is presented in a separate report by Zavala et al. [8].

2. Experimental description

2.1. Mobile laboratory

The mobile laboratory was equipped with a combination of research grade and commercial instrumentation possessing sufficient time response and sensitivity to characterize the particle and gas phase composition of dilute exhaust plumes. This mobile lab has been described in detail previously [5] so only those details relevant to the present study are discussed here. On-road vehicle emission characterization was performed by driving in heavy traffic corridors or "chasing" specifically targeted vehicles [9,10]. In either mode of operation, the partially diluted exhaust plumes are sampled through a common sample inlet that protrudes through the bulkhead of the truck, directly above the driver. This flow (20 SLM) was isokinetically split to provide flows to the particle and gas phase instruments. Approximately every 20 min the sample line was flooded with zero air to provide instrument zeroes and also served as a recognizable event to time synchronize all of the instruments.

2.2. PTR-MS description

A commercial version of the PTR-MS (Ionicon Analytik) was modified to handle the high impact shocks and thermal loads experienced within the mobile laboratory during on-road operation. To mitigate the shock and vibration, the instrument rack and drift tube mass spectrometer assembly were individually shock mounted using a combination of rubber bushings and coil spring technologies. The orientation of the large turbo-molecular pump was changed from horizontal to vertical by use of a 90° elbow. This orientation change was made on basis of numerous peer recommendations that turbo pumps can better tolerate impact shock when mounted vertically. The original turbo pump equipped with a magnetic top bearing malfunctioned on the first drive and was replaced with a fixed bearing 250 l/s Varian Navigator 301 turbo pump. The original small 33 l/s turbo pump handled the road shock without incident, but required a reduction in its rotational speed in order to handle the high internal mobile lab temperatures.

The PTR-MS utilized in this study is one of the earliest production models and the original sample inlet flow controller was replaced with a pressure controlled inlet. This modification significantly decreases the residence time of the sample in the inlet line and allows the PTR-MS to track rapidly changing concentrations within the exhaust plumes [11]. This modification is described more completely elsewhere [11]. The inlet line was constructed using small internal diameter PFA Teflon tubing and fittings except the stainless steel fine metering valve that was used to create the critical pressure drop. The nominal total volumetric flow rate was approximately 300 sccm which minimizes the sample residence time within the inlet line. The drift tube pressure was nominally 1.9 mbar at 295 K and flow calculations predict that the residence time of the gas sample within the drift tube will be about 1.6 s.

For the on-road measurements, the PTR-MS was programmed to monitor 12 masses at 0.1 s per mass plus the drift tube pressure and temperature, resulting in a measurement cycle of just less than 2 s. The ions monitored included the reagent ions H_3O^+ (mass 21, ^{18}O isotope) and $H_3O^+(H_2O)$ (mass 39 ^{18}O isotope) and the following sample ions: mass 33 – methanol, mass 45 – acetaldehyde, mass 57 – sum of MTBE and butenes (C_4H_8), mass 59 – acetone, mass 61 – ethyl acetate fragment, acetic acid, mass 79 – benzene, mass 89 – ethyl acetate, mass 93 – toluene, mass 107 – C2-benzenes (sum of xylene isomers, ethylbenzene, and benzaldehyde) and mass 121 – C3-benzenes (sum of C_9H_{12} isomers and C_8H_8O isomers). The ion measurements at mass 61 and mass 89 were monitored primarily as part of an urban plume mapping study [12,13]. Ambient air was sampled for 600 measurement cycles followed by 60 cycles of instrumental background measurements determined by diversion of the sample flow through a Platinum catalyst (Shimadzu) heated to 400 °C that provided a VOC free gas stream. The instrumental background was non-zero in most cases and the reported

concentrations reflect the difference between the ambient and instrument background signals.

Trace gas concentrations can be determined from the measured ion signals using equations derived from simple reaction kinetics [6] or from measured or estimated calibration response factors. The accuracy of the concentrations derived directly from reaction kinetics are dependent on the validity of the value of the reaction rate constant used, and also on how well the measured reagent ion intensities reflect their actual ion distributions within the drift tube. Better quantitative accuracy can be achieved by the use of calibration standards. In this study, calibrated responses are determined through dilution of a certified high pressure gas mixture (Apel–Reimer) and the evaluated calibration factors are related to the volumetric mixing ratio (VMR) as shown in Eq. (1) [11] where I_{RH^+}, $I_{H_3O^+}$ and $I_{H_3O^+(H_2O)}$ represent the respective product and reagent ion intensities, T is the drift tube temperature, P the drift tube pressure, S_R the overall sensitivity factor and X_R compensates for reaction efficiency of the $H_3O^+(H_2O)$ reagent ion:

$$\mathrm{VMR_R} = \left(\frac{1}{S_R}\right)\left(\frac{I_{RH^+}}{I_{H_3O^+} + X_R \times I_{H_3O^+(H_2O)}}\right)\left(\frac{T^2}{P^2}\right) \quad (1)$$

The sensitivity factors, S_R, are derived from the slopes of four-point dilution curves obtained by plotting $\frac{I_{RH^+}}{I_{H_3O^+}+X_R \times I_{H_3O^+(H_2O)}}$ versus $\mathrm{VMR_R}\left(\frac{P^2}{T^2}\right)$. A summary of the sensitivity factors measured during the MCMA field campaign is shown in Fig. 1. The X_R terms, which account for the difference in the reactivity between H_3O^+ and $H_3O^+(H_2O)$ were determined separately at the conclusion of the campaign by empirically selecting a value of X_R that minimized the dependence of S_R to changes in the observed reagent ion distribution $\frac{I_{H_3O^+}}{I_{H_3O^+}+I_{H_3O^+(H_2O)}}$. Negative X_R values indicate that some declustering of $H_3O^+(H_2O)$ to H_3O^+ occurs within the expansion region of the instrument and are expected only for those compounds which do not react with $H_3O^+(H_2O)$. While the negative X_R values adequately minimized the dependence of S_R on the observed reagent ion distribution, it is now known that the negative X_R values for toluene, *p*-xylene and 1,2,4-trimethylbenzene reported in Table 1 do not accurately reflect the reactivities of these compounds with $H_3O^+(H_2O)$. These incorrect X_R values do not significantly compromise the accuracy of the determinations reported here because the intensity of the clustered reagent ion $H_3O^+(H_2O)$ was essentially the same for both the ambient sampling and calibration experiments. Using a 600 V applied field at 1.9 mbar and 300 K or E/N = 145 Td, $H_3O^+(H_2O)$ averaged about 11% of the total reagent ion intensity and varied from a low of 8% to a high of 18%. We estimate that at the highest levels of $H_3O^+(H_2O)$ that the concentrations determined for the C3-benzenes could be overestimated by 15%. The respective errors in the C2-benzenes and toluene will be progressively smaller because these species are less reactive towards $H_3O^+(H_2O)$. Campaign averaged sensitivity factors have been used to compute the reported concentrations and are shown in Table 1. The ion detected at mass 57 has been quantified as if it originated solely from the ion-

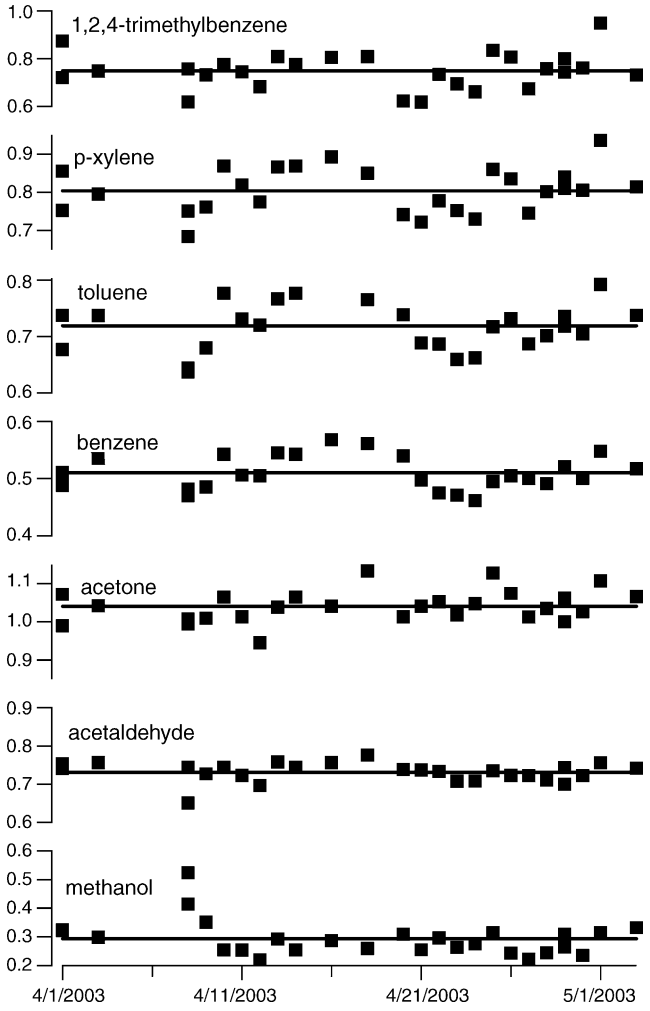

Fig. 1. PTR-MS calibration factors found throughout the campaign. The squares represent individual calibration experiments and the line represents the average value used in data analysis.

ization of methyl tertiary butyl ether (MTBE) and the response factors reported on the basis that $S_{MTBE} = (K_{cMTBE}/k_{c,acetone})\, S_{acetone}$ where the k_{cMTBE} is taken to be 2×10^{-9} cm^3/s and the k_c for acetone 2.3×10^{-9} cm^3/s is the calculated proton transfer reaction rate constant assuming an ion energy of 0.2 eV [6,14,15]. For the case of the C2-benzenes and C3-benzenes it has been assumed that all of the structural isomers have the same response factors as their respective calibration compounds *p*-xylene and 1,2,4-trimethylbenzene. This latter assumption relies on the fact that the calculated reaction rate constants for different C2-benzene isomers vary by less than 10% and that the limited set reported for the C3-benzenes exhibit similar behavior [16]. Also included in Table 1, for comparison, are the sensitivity factors calculated as counts per second (cps) per ppbv normalized to 1 million cps reagent ion (ncps) at 2.4 mbar and 300 K.

Limits of detection are defined in this study as three times the signal to noise ratio (S/N), where the S/N is taken as the 1σ level of scatter in the background concentration measurements. These limits of detection are included in Table 1 and are based on 0.1 s measurement time and range from 5.1 ppb for methanol to 1 ppb for toluene. Because the reported concentrations reflect

Table 1
Summary of calibration information

Compound	Mass	S_R (S.D.)	X_R	Calc ncps[a] (2.4 mbar)	Lit ncps (2.4 mbar[b])	LD[c] (ppbv)
Methanol	33	0.30 (0.05)	0.38	19.2	23.6	5.1
Acetaldehyde	45	0.73 (0.02)	0.6	46.7	26.6	3.9
Mass 57[d]	57	0.91	0.5	58.2		3.4
Acetone	59	1.05 (0.04)	0.7	67.2	64.0	1.6
Benzene	79	0.51 (0.03)	−0.4	32.6	33.8	1.6
Toluene	93	0.72 (0.04)	−0.4	46.7	45.4	0.93
p-Xylene	107	0.80 (0.06)	−0.4	51.2	18.7	1.4
1,2,4-Trimethylbenzene	121	0.75 (0.08)	−0.4	48.0	30.2	1.7

Compound identification, measured calibration factors, calculated normalized counts per second (ncps) at 2.4 mbar, ncps from literature reference, and limits of detection.

[a] Counts per second normalized to 1 ppbv per million reagent ions calculated at 2.4 mbar and 300 K using the expression $\text{ncps} = 1 \times 10^6 \times S_R \times (P^2/T^2)$.

[b] From de Gouw et al. [19].

[c] Determined as three times the S/N standard deviation.

[d] Mass 57 sum of MTBE and C_4H_8 isomers see text for details.

the difference between ambient and background concentration measurements, the higher limits of detection for methanol and acetaldehyde reflect the higher persistent background levels within the PTR-MS. Compounds with near zero background ion counts like benzene and toluene have more favorable limits of detection.

2.3. GC-FID measurements

During the MCMA-2003 study, 6-l stainless steel canisters were filled using a commercial Xon Tech Model 910PC sampler. Integrated samples were collected for 1- or 3-h periods throughout a 24-h day. After collection, canisters were delivered to the Washington State University (WSU) field laboratory at CENICA for gas chromatographic analysis. Analyses were performed within 24 h on an Hewlett Packard 5890 GC equipped with FID detector. The GC system had a DB-1 fused silica capillary column (J & W Scientific) for the separation of VOC compounds. A cryotrap attached to the gas chromatograph via a six-port gas-sampling valve (Valco Inst. Co. Inc.) was used for concentrating the organic compounds prior to injection on the GC column. Normally, 300 ml of air was passed through the freeze-out trap, which was maintained at −186 °C (liquid oxygen). Hydrogen at 1 $cm^3\,min^{-1}$ was employed as the carrier gas with the DB-1 fused silica capillary column system. Optimum separation was achieved using an oven temperature ramp from −50 to 150 °C at 4° min^{-1}. GC peaks were identified by comparing their retention times with known standards. Hydrocarbon concentrations were determined by the ratio of the FID response for each peak to the response recorded for a known concentration of 2,2-dimethylbutane. The concentration of the 2,2-dimethylbutane standard was assigned through comparison with a NIST-purchased propane standard reference material (SRM).

2.4. CO_2 measurements

A Licor 6262 non-dispersive infrared absorption instrument was used to measure the CO_2 concentration. Since CO_2 serves as the dilution tracer, all other measurement time bases are adjusted to correlate with that of CO_2 using the zero air purges for time synchronization.

3. Results and discussion

3.1. PTR-MS time response

On-road exhaust emission characterization experiments are based on the premise that CO_2 can be used as an internal tracer and that the exhaust dilution factor is contained in the change in CO_2 concentration [5]. Experimentally this requires that the time response and sensitivity of the PTR-MS measurements be high enough to follow the rapidly changing concentrations within the exhaust plume. Fig. 2 provides a representative on-road profile of toluene and CO_2. Inspection of this figure shows that the CO_2 and toluene signals are highly correlated and that the PTR-MS instrument appears to have sufficient time response for characterizing the individual plumes. The zero air purges used to match the time base of the two instruments are visible in Fig. 2 at 6:10:45 and 6:31:45. Correlation of PTR-MS time base to that of CO_2 signal is critical to interpreting these data. Elevated PTR-MS signals with concomitant rise in CO_2 is indicative of fossil fuel combustion.

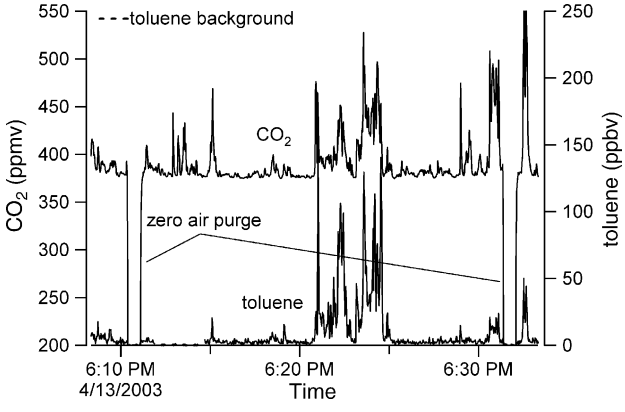

Fig. 2. On-road data for toluene and CO_2 showing time correlation of the signals and the zero air purges used for time synchronization.

3.2. Interpretation of mass spectral assignments

The PTR-MS has not previously been applied to the study of vehicle tail pipe emissions and in the following section each of the mass assignments is examined in detail. Where possible, the concentrations derived from the PTR-MS measurements are directly compared to ambient air samples collected in collocated canisters that have been analyzed by GC-FID. For components that were not measured in the canister samples the results of this study are discussed relative to previously published PTR-MS studies.

3.2.1. Mass 33

The ion at mass 33 is attributed to the presence of methanol. This ion is unique to methanol and there are no known hydrocarbon compounds which interfere with this measurement [17]. Methanol was not measured in the canister samples in this study, but previous studies have shown excellent correlation between the PTR-MS derived concentrations with that of FTR-IR [18] and GC–MS [19]. Methanol is observed to be a tailpipe emission product, but also has significant non-exhaust vehicle sources. Windshield wiper fluids contain methanol as an active ingredient. In-use antifreeze coolants show the presence of methanol either as a contaminant or a breakdown product. These other sources can be distinguished from tail pipe emissions since they are not correlated with the CO_2 measurements.

3.2.2. Mass 45

The ion at mass 45 is attributed to the presence of acetaldehyde. There are several small interferences that are known to effect the quantification of acetaldehyde. Ethylene glycol, the major ingredient of vehicle antifreeze, fragments upon ionization to produce an ion at mass 45. Generally the vapor pressure of ethylene glycol is low enough that it does not contribute significantly to the signal at mass 45 except for the case of overheated vehicles. In most cases the interference from ethylene glycol can be resolved from exhaust emitted acetaldehyde on the basis of the CO_2 signal. Another minor interference is from CO_2 [17], which apparently contributes ion intensity to this mass through an endothermic proton transfer reaction in the expansion region to form the HCO_2^+ ion (mass 45). In a separate laboratory study the CO_2 contribution to the mass 45 signal has been evaluated using calibrated CO_2 standards. It was determined that 1 ppmv CO_2 produces a response equivalent to 1 pptv acetaldehyde. The perturbation due to CO_2, can be easily corrected for since CO_2 concentrations are known, but have not been made since these corrections are small in these on-road studies. For example, an exhaust plume characterized by a 100 ppm change in CO_2 would only contribute an additional 0.1 ppb to measured concentration. It has been reported that the alkenes and ozone can react on stainless steel surfaces to produce acetaldehyde [20]. This latter perturbation was found to be important when very low levels of acetaldehyde were being measured and is not thought to be important in this urban airshed where fairly high levels of acetaldehyde are typically found. In previously reported PTR-MS studies the derived acetaldehyde concentrations compared favorably with GC–MS measurements when acetaldehyde mixing ratios exceeded 1–2 ppbv [20,21]. The acetaldehyde levels in the roadway experiments usually exceed 1–2 ppbv and thus we consider that these acetaldehyde measurements are not significantly perturbed by the aforementioned interferences.

3.2.3. Mass 57

Several major gasoline vehicle exhaust emission components are expected to contribute to the ion signal at mass 57, including MTBE and the C_4H_8 (butene) isomers. MTBE is considered to be an important exhaust emission component because it is used as an additive in reformulated fuels sold in the MCMA [1,22] and that emissions measured from vehicles using fuels containing MTBE reflect the presence of this fuel additive [23]. The butene isomers are also significant gasoline vehicle exhaust components [23]. The butenes react to form protonated molecular ions at this mass while greater than 95% of the MTBE nascent proton transfer reaction products fragment to the mass 57 ion. Acrolein, an important air toxic, is thought to be only a minor component in gasoline vehicle exhaust [23] and is not expected to contribute significantly to the mass 57 ion signal. There are other components such as the higher order alkenes (>C6) [24] and higher order alkanes (>C7) [25,26] that react with H_3O^+ to produce ion fragments at mass 57. Reactions of O_2^+ with higher order alkanes and alkenes are also known to form product ion fragments at mass 57 [24]. The latter reactions are generally unimportant and can be ignored because O_2^+ represents only about 2% of the total reagent ion intensity. The concentrations of MTBE and butenes are expected to be much greater than those of acrolein and the higher order alkenes and alkanes in gasoline vehicle exhaust [23] so that these compounds are not expected to interfere significantly. Based on vehicle exhaust source profiles derived from MCMA tunnel studies [27] it was initially assumed that MTBE would be the major contributor to the ion signal at mass 57 and the ion signal was quantified on this basis. It is now recognized that the concentrations derived from ion intensity measurements at mass 57 predominately reflects the sum of the butene isomers and MTBE. While the concentrations derived here were calculated assuming a k_{cMTBE} of 2×10^{-9} cm^3/s, and the proton transfer reaction rate coefficients for the different isomeric butenes are not so different and range from 1.7×10^{-9} to 1.8×10^{-9} cm^3/s [16] so that using a weighted averaged sensitivity factor would have only a small effect on the reported concentrations. Fig. 3a shows a time series plot of PTR-MS mass 57 concentration along with the MTBE and C_4H_8 isomer concentrations determined by GC-FID for the La Merced stationary sampling site, which is an urban core site that is heavily influenced by vehicle emissions. The GC-FID results have been shown as a bar which has been shaded to show the relative contributions of MTBE and the isomeric butenes. While the bars obscure some of the detail in Fig. 3a, the correlation between the two data sets can be more clearly seen in Fig. 3b where the PTR-MS concentration has been averaged over the time period that the canisters were filled. The correlation plot shows that the PTR-MS derived concentrations are in excellent agreement with corresponding GC-FID results, which lends credence to our assertion that MTBE and the C_4H_8 isomers are the dominant components being detected at mass 57 by the PTR-MS.

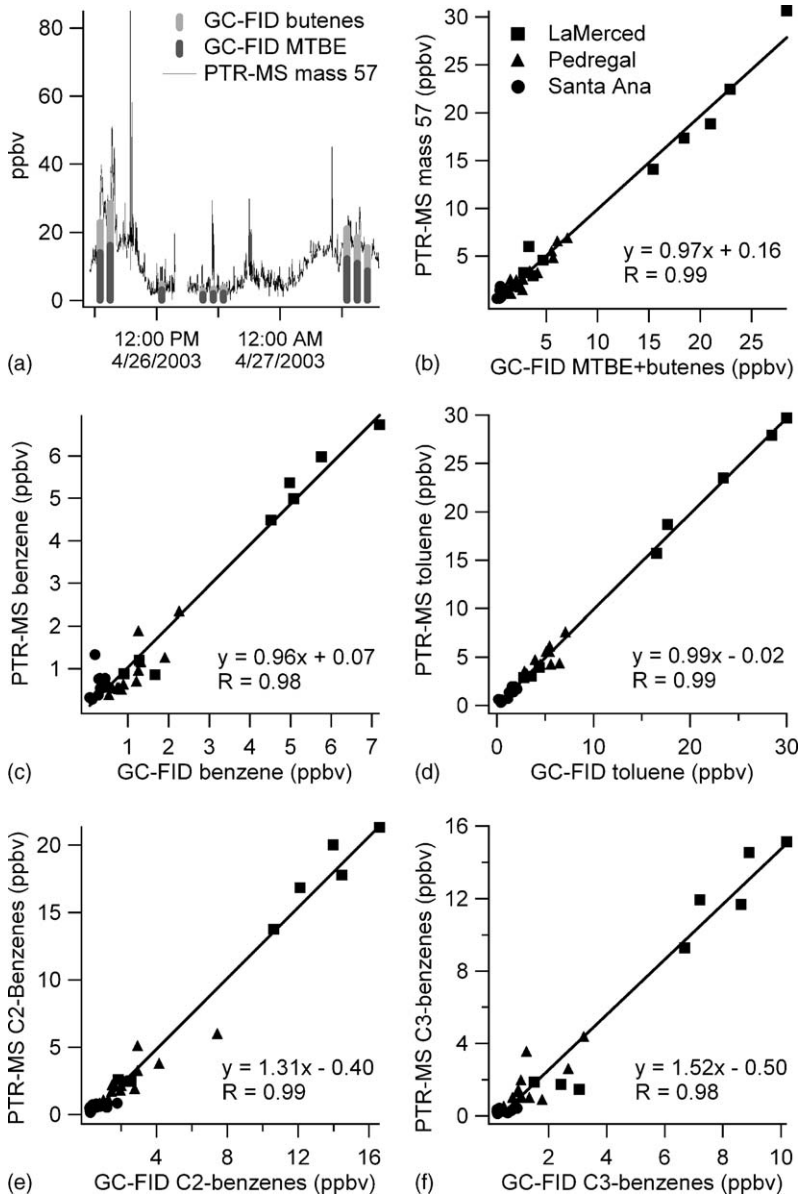

Fig. 3. Time series plot (a) of the mass 57 concentration where the GC-FID results for butenes and MTBE have been overlayed. The shading of the bar shows the relative contributions of MTBE and the butenes. Correlation plots of the PTR-MS and GC-FID results from the same air mass for (b) sum of MTBE and the isomeric butanes, (c) benzene, (d) toluene, (e) C2-benzenes and (f) C3-benzenes. The various symbols represent data from different locations, while the line is the least squares regression.

Diesel vehicles have a much different chemical speciation [28–30] than that of gasoline vehicles, but because of their low hydrocarbon emission factors [28,29] are not expected to alter the mass 57 signature that is dominated by gasoline vehicle emissions. Several studies have examined diesel exhaust using H_3O^+ chemical ionization techniques and each one provides a substantially different interpretation of the ion signals [25,31]. The PTR-MS study is most relevant to the discussion here, and in that report all of the intensity observed at mass 57 was attributed to the fragmentation of large alkanes [25]. We have also examined the exhaust of a stationary diesel vehicle with our PTR-MS and observe a mass spectrum that is very similar to that reported by Jobson et al. [25]. Using the report by Schauer et al. [29] as a guide for interpreting the PTR-MS mass spectrum of diesel exhaust we conclude that the mass 57 ion receives significant intensity from a wide variety of neutral components including the isomeric butenes, acrolein, higher order alkenes and alkanes. In the cases where diesel exhaust plumes are intercepted and signal is detected at mass 57 we do not associate any specific neutral components with this ion.

3.2.4. Mass 59

The ion signal at mass 59 receives intensity contributions from the presence of acetone, propanal, and glyoxal. Schauer et al. [23] report that all three species are present at significant fractions in gasoline powered vehicles without catalytic converters, with mole fractions of 46%, 32%, and 22% for propanal, acetone, and glyoxal, respectively. Quantification of the mass 59

ion signal was done using the acetone calibration factor and the resulting concentration should be considered as a lower limit to the sum of the species since the reaction rate constant for glyoxal is much smaller than that of acetone and propanal [16]. These compounds were observed to be only minor exhaust emission products.

3.2.5. Mass 61

The ion signal at mass 61 was monitored primarily as a fragment ion of ethyl acetate as part of an urban plume dispersion study [12,13]. However, this ion is typically associated with acetic acid [18,19,25] and should reflect the presence of this compound when the mobile laboratory was not being influenced by strong local sources of ethyl acetate. The ion signal at mass 61 was found to be unaffected by on-road vehicle exhaust sampling encounters. On this basis we would conclude that acetic acid is not a vehicle exhaust emission product. This conclusion appears to be inconsistent with a recent study where acetic acid was identified as a diesel exhaust emission component [25], but probably reflects that the concentration of acetic acid in the diluted exhaust plumes encountered in this study was below our detection limit which is estimated to be on the order of 4 ppb.

3.2.6. Mass 79

This ion is predominately formed via a proton transfer reaction with benzene. Higher order mono-substituted benzenes such as ethylbenzene and the propylbenzene isomers fragment within the PTR-MS to produce ions at mass 79 and thus interfere with quantification of benzene. The contributions from benzene, ethylbenzene and propylbenzene to the total mass 79 concentration or VMR are given in Eq. (2):

$$[M79] = [\text{Benz}] + \frac{S_{\text{EtBenz}}}{S_{\text{Benz}}}\text{BF}_{\text{EtBenz}}[\text{EtBenz}] + \frac{S_{\text{PrBenz}}}{S_{\text{Benz}}}\text{BF}_{\text{PrBenz}}[\text{PrBenz}] \quad (2)$$

where [M79] represents the VMR derived from the total mass 79 ion intensity assuming it originated solely from benzene. The terms [Benz], [EtBenz] and [PrBenz] represent the actual VMRs of the respective species. The contributions from ethyl and propylbenzene are weighted by the ratio of the ionization efficiencies (S_x/S_{Benz}) and the fraction (BF_x) of the mass 79 ion product that each produces upon ionization. Under the experimental conditions used in this study, ethylbenzene forms 68% mass 107 and 32% mass 79, while propylbenzene forms 36% mass 121 and 64% mass 79. Evaluation of the individual concentrations of ethylbenzene and propylbenzene is not possible with the PTR-MS since there are other C_8H_{10} and C_9H_{12} isomers present in the ambient air mass. The sum of all of the C_8H_{10} isomers is generally referred to as the C2-Benzenes while the sum all of the C_9H_{12} isomers represent the C3-Benzenes. Fortunately it has been observed that ethylbenzene is a reasonably constant fraction of the C2-Benzenes throughout the MCMA as shown in Fig. 4. Propylbenzene exhibits similar behavior. Substitution of the detection sensitivities, the product branching fractions and [EtBenz] = 0.182 × [C2Benz] and

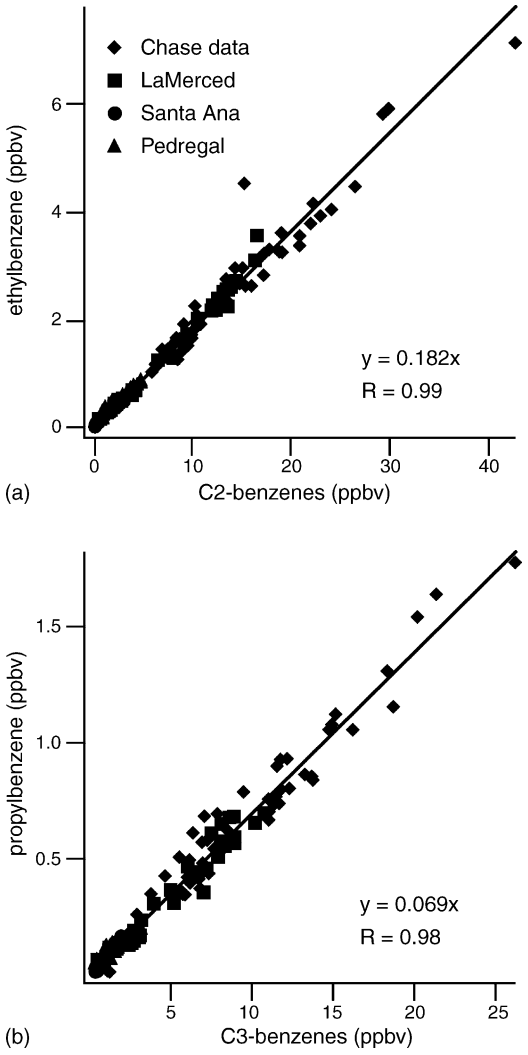

Fig. 4. GC-FID measurements from canister samples taken from different locations throughout the MCMA: (a) ethylbenzene concentration vs. the total C2-benzene concentration; (b) propylbenzene concentration vs. the total C3-benzene concentration.

[PrBenz] = 0.069 × [C3Benz] allows us to derive an algorithm, Eq. (3), to correct for the contributions of these components to the benzene signal:

$$[\text{Benz}] = [M79] - 0.092 \times [\text{C2Benz}] - 0.065 \times [\text{C3Benz}] \quad (3)$$

Fig. 3c shows the correlation between the PTR-MS corrected benzene concentrations and the GC-FID benzene measurements made at several different stationary sampling sites. The agreement between the two methods is very good and serves to validate that reliable benzene concentrations can be derived from the PTR-MS measurements. Accurate benzene measurements are important in the present study, as the benzene to toluene ratio is an important indicator in determining whether a vehicle has a functioning exhaust treatment system [32,33].

3.2.7. Mass 89

The ion signal at this mass reflected the presence of ethyl acetate and was monitored as part of an urban plume dispersion

study [12,13]. This mass assignment is specific to this particular application and was confirmed by GC analysis of ambient air samples captured in canisters at the emission source. It is noted that this ion signal was totally quiescent except for when the mobile laboratory intercepted an ethyl acetate solvent plume. This result provides strong evidence that ethyl acetate is not present to any significant extent in vehicle exhaust.

3.2.8. Mass 93

The ion at mass 93 is attributed to the presence of toluene. Certain terpenes like α- and β-pinene produce a small amount of fragment ion at mass 93 [19]. The contributions from these biogenic species to the ion signal at mass 93 are expected to be insignificant in the MCMA air masses analyzed. Fig. 3d shows that the PTR-MS and GC-FID measurements made at several stationary sites are in excellent agreement with one another. Toluene is considered to be the best and most reliable of the PTR-MS measurements reported here. Toluene is observed to be a dominant exhaust emission product from gasoline vehicles.

3.2.9. Mass 107

The ion signal observed at mass 107 reflects the sum of the xylene isomers and ethylbenzene (C2-benzenes) plus benzaldehyde. As noted in the experimental section, quantification of the C2-benzenes assumes that the *p*-xylene calibration factor is appropriate for all of the components. The calculated proton transfer reaction rate constants are all very similar for ethylbenzene [16] and the xylenes [16] and on this basis the use of a single component calibration response is appropriate. If we assume that the sensitivity factors scale on the basis of the value of the reaction rate constant, then benzaldehyde would be expected to have a higher sensitivity factor. However, it has been reported in a GC/PTR-MS study that ethylbenzene has a higher response factor (20.7 ncps/ppbv), and benzaldehyde a lower response factor (7.9 ncps/ppbv) compared to *p*-xylene (15.2 ncps/ppbv) [26]. These calibration factors for the individual C2-isomers show a much greater range of variability than would have been expected on the basis of differences in the reaction rate constants and would suggest the use of a weighted averaged sensitivity factor rather than the single component derived value employed here. Fig. 3e shows the correlation plot for the mass 107 signal (C2-benzenes plus benzaldedyde) from the PTR-MS versus the C2-benzenes as measured by GC-FID. The slope of this correlation plot shows an overestimation by PTR-MS of approximately 30%. One factor contributing to the error is the fact that benzaldehyde is measured at mass 107 by the PTR-MS, but was not measured by the GC-FID. However, it is noted that this factor alone probably does not account for all of the discrepancy as automotive exhaust emission studies indicate that the benzaldehyde contribution might add 5% to the overall measurement [23]. These measurements may be additionally compromised under high humidity conditions because of inaccurate compensation of the reactivity of these compounds with $H_3O^+(H_2O)$. In other PTR-MS and GC/MS intercomparison experiments involving the C2-benzenes, one study indicated very good agreement between the two methods [21] while a second study [34] reported results very similar to that observed here. The C2-benzene measurements have greater uncertainty and may overestimate the true concentrations of these species. The C2-benzenes are observed to be dominant exhaust emission components of gasoline vehicles.

3.2.10. Mass 121

There are eight C_9H_{12} isomers and five C_8H_8O isomers that contribute to the ion signal at mass 121. This collection of compounds is referred to as the C3-benzenes, although it actually represents the C3-benzenes plus C_8H_8O aromatic aldehydes and ketones. Concentrations have been calculated assuming that the calibration factor for 1,2,4-trimethylbenzene is appropriate for all of the isomers. Similar to mass 107, larger errors are expected for the quantification of this collection of compounds. Reaction rate coefficients for the C_9H_{12} isomers that have been tabulated are quite similar, while those of the C_8H_8O compounds are somewhat larger. Fig. 3f shows that the concentrations derived from the PTR-MS are 50% larger than those determined by GC-FID. A portion of this error may be attributed to omission of C_8H_8O isomers from the GC-FID data, but it seems unreasonable to attribute all of the discrepancy to this factor. Gasoline automobile emission studies report that the three tolualdehyde isomers may contribute an additional 10% to the overall C3-benzene measurement [23]. These measurements may be additionally compromised under high humidity conditions because of inaccurate compensation of the reactivity of these compounds with $H_3O^+(H_2O)$. Other PTR-MS and GC/MS intercomparison studies involving the C3-benzenes seem to indicate that the PTR-MS results are consistently high. Until the source of uncertainty of these measurements can be identified we consider the PTR-MS measurements more as a proxy for the C3-benzenes rather than an exact measurement.

3.3. Vehicle exhaust characterization experiments

A major goal for deploying the PTR-MS on-board the mobile laboratory in the MCMA field campaign was aimed at the study and characterization of selected hydrocarbon exhaust emissions of vehicles operated under real-world driving conditions. Zavala et al. [8] provide a complete analysis of the hydrocarbon emission measurements from mobile sources in the MCMA. In this manuscript specific case examples of hydrocarbon exhaust emission measurements made by the PTR-MS from different engine types are highlighted, and include gasoline vehicles with and without exhaust treatment systems and a diesel vehicle. Classification of the emission profiles is based on following general criteria, video images and researcher data log notes recorded during the chase event and corroborating measurements from other instruments. Video records indicated that only the targeted vehicle was in front of the mobile laboratory during the reported chase segments. Fig. 5 shows selected 1–2 min chase segments that are representative of each of the vehicle types and also have similar excess CO_2 concentrations. The scaling of the axes are the same for each of the different compounds to help illustrate the different emission characteristics of the profiled vehicles. The shaded regions indicate the specific plumes that are analyzed and discussed below.

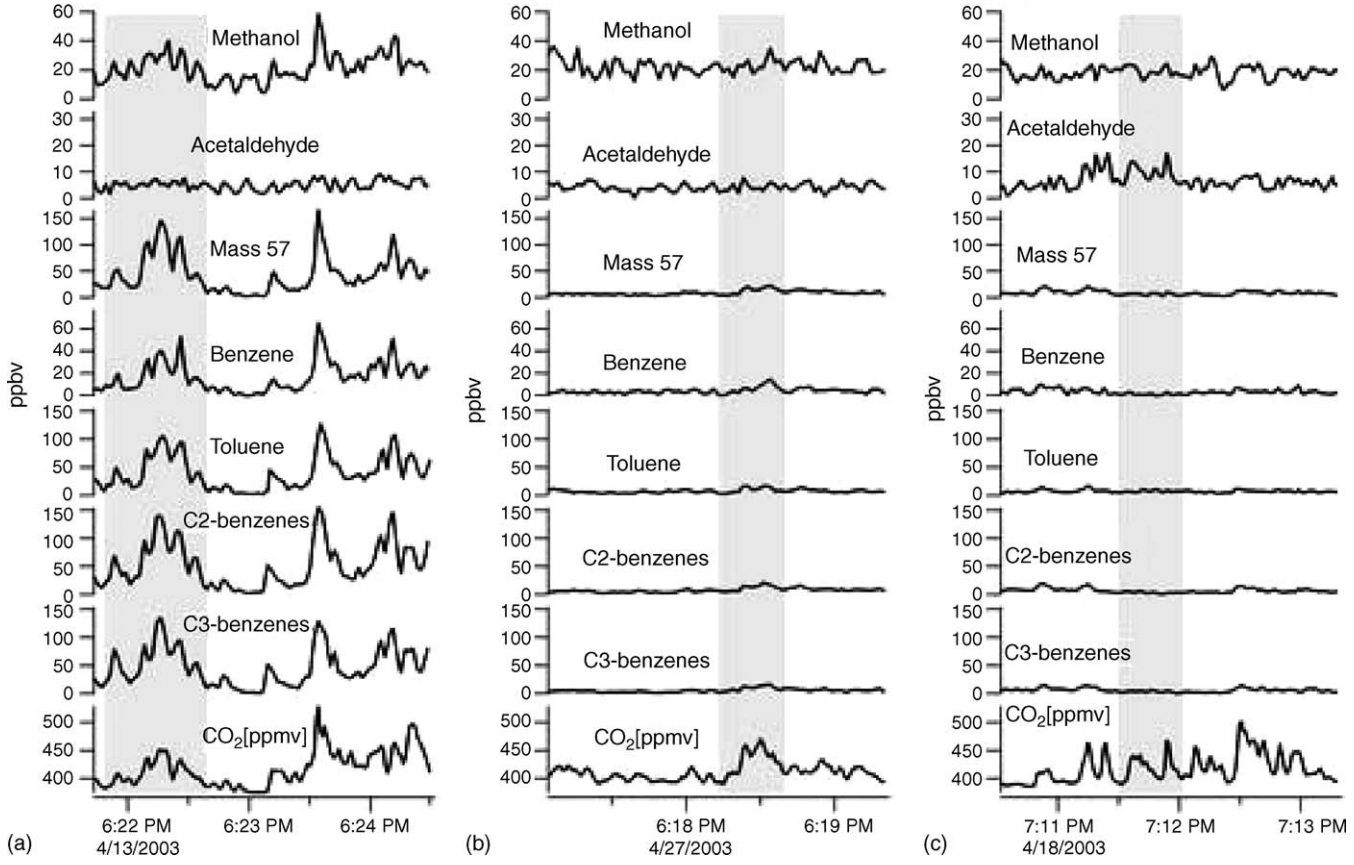

Fig. 5. Selected hydrocarbon and CO_2 emission time series measurements of representative chase events: (a) gasoline vehicle without an operational catalytic converter; (b) gasoline vehicle with an operational catalytic converter; (c) heavy duty diesel charter bus. Shaded areas indicate the plumes analyzed in Fig. 6.

Fig. 5a shows a chase segment for an older (early to mid 1990s) Chevrolet Suburban that was followed at low speeds (5–20 mph) within a city park. This vehicle is equipped with a gasoline engine (most likely a large displacement eight cylinder engine) and on the basis of the large concentrations of exhaust products measured has been classified as a vehicle without a functioning catalytic converter. For this vehicle all of the components except acetaldehyde and those not plotted (masses 59, 61 and 89) are observed in high concentration and are highly correlated with the CO_2 measurement. The method used to quantify these emissions is determined from a correlation plot of the emission analyte concentration versus the CO_2 concentration where the slope represents the emission ratio [5]. Fig. 6 shows the correlation plot for the toluene and CO_2 measurements made over the times indicated by the shading in Fig. 5. In the case of the Chevrolet Suburban the emission ratio of toluene was determined to be 1.4 ppbv toluene per ppmv CO_2 or 1.4×10^{-3} mole toluene per mole of CO_2. Emission ratios were determined from the slopes of similar plots for each of the other components and are reported in Table 2. For comparison emission ratios estimated from emission factors reported for cars tested using an urban FTP cycle are also included in Table 2. Except for acetaldehyde the emission ratios derived from this single plume event are consistent with that reported by Schauer et al. [23] for vehicles without operational catalytic converters. Acetaldehyde was observed to be only a minor emission product from this vehicle essentially indistinguishable from the ambient background. For vehicles without operating catalytic converters Schauer et al. [23] observed that the acetaldehyde emissions were slightly greater than the corresponding benzene emissions. Had this been the case here the acetaldehyde

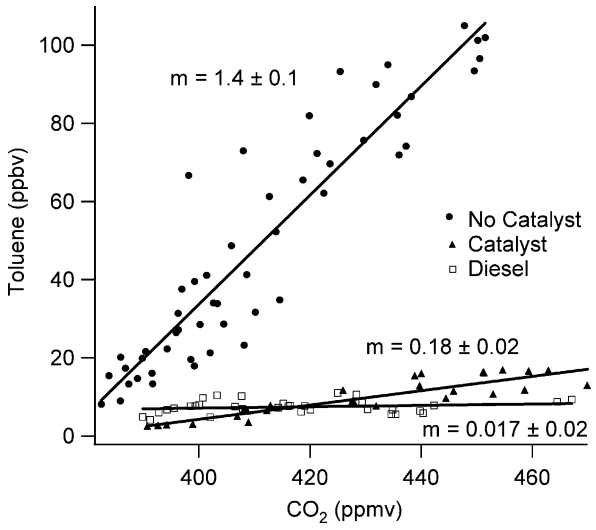

Fig. 6. Toluene and CO_2 correlation scatter plots for the plume data indicated by the shaded regions in Fig. 5. Emission ratios are evaluated from the slope of plots.

Table 2
Summary of the emission ratio (mole of compound per mole CO_2) measurements of the selected plumes in Fig. 5

Compound	Gasoline engine without operational catalyst		Gasoline engine with operational catalyst		Heavy Duty Diesel Charter Bus	
	Fig. 5	Schauer et al.[a] [23]	Fig. 5	Schauer et al.[b] [23]	Fig. 5	Cocker et al. [28]
Methanol	2.9×10^{-4}	–	NR	–	1.6×10^{-5}	–
Acetaldehyde	1.8×10^{-5}	6.4×10^{-4}	2.4×10^{-5}	1.7×10^{-5}	1.2×10^{-4}	4×10^{-5}
Benzene	5.3×10^{-4}	5.6×10^{-4}	1.1×10^{-4}	2.9×10^{-5}	1.2×10^{-5}	2.9×10^{-6}
Toluene	1.4×10^{-3}	2.4×10^{-3}	1.8×10^{-4}	4.4×10^{-5}	1.7×10^{-5}	1.4×10^{-6}
C2-benzenes[c]	1.6×10^{-3}	2.6×10^{-3}	2.0×10^{-4}	4.3×10^{-5}	1.1×10^{-5}	1.8×10^{-6}
C3-benzenes[d]	1.4×10^{-3}	1.4×10^{-3}	1.6×10^{-4}	2.5×10^{-5}	3.3×10^{-5}	–
Mass 57[e]	1.9×10^{-3}	2.6×10^{-3}	2.2×10^{-4}	7.4×10^{-5}	–	–

[a] Emission ratios are estimated from the reported emission rates assuming 5 km/l, fuel density of 0.75 g/ml and 3140 g CO_2/kg of fuel.
[b] Emission ratios are estimated from the reported emission rates assuming 10 km/l, fuel density of 0.75 g/ml and 3140 g CO_2/kg of fuel.
[c] Sum of C_8H_{10} isomers plus C_7H_6O.
[d] Sum of C_9H_{12} isomers plus C_8H_8O isomers.
[e] Sum of MTBE and C_4H_8 isomers.

emissions would have been clearly observable for this vehicle. The ratio of acetaldehyde to benzene observed here of 0.034 is more similar to that (0.063–0.073) observed in a dynamometer study involving 1991–1996 fleet cars from the MCMA by Schifter et al. [22].

Fig. 5b shows a chase segment for a newer small sedan that was intercepted as it was pulling away from a traffic light and represents a gasoline vehicle that appears to have a properly functioning catalytic converter. Only the single plume centered at 6:18:30 can be ascribed to this vehicle. The emission ratios determined for this vehicle except for acetaldehyde are substantially reduced relative to that shown for the gasoline vehicle without a catalytic converter. The reduced molar emission ratios and the elevated benzene to toluene ratio (0.61) are consistent with a vehicle having a properly functioning catalytic converter [23,35]. The molar emission ratios for benzene, toluene, C2-benzenes, C3-benzenes and mass 57 (MTBE plus butenes) for this vehicle are observed to be 3–6 times larger than that reported by Schauer et al. [23] for catalyst-equipped gasoline-powered motor vehicle tailpipe emissions. Given that the plume recorded in Fig. 5b for this vehicle represents an acceleration plume, higher emissions might be expected [33].

Fig. 5c shows a chase segment involving a diesel charter bus. Diesel vehicles generally have very low hydrocarbon emissions and are difficult to profile for this reason. Video records and corroborating particle emission measurements indicate that this was a very clean chase event. Diesel engines have significant particle emissions [36,37] and these measurements indicated that the exhaust from the targeted charter bus was being continuously sampled over the entire chase sequence. Considerable variability is noted in the hydrocarbon traces associated with this vehicle. For the shaded plume event between 7:11:30 and 7:12:00 it is seen that the acetaldehyde signal clearly tracks the corresponding CO_2 trace and that the other hydrocarbon emissions are very low. This can be contrasted to the plume event starting about 7:12:30 and lasting to 7:13:00, where the aromatic emission components appear more significant while the acetaldehyde emission is lower. Emission ratios for the shaded plume event are shown in Table 2. It is noted that while the acetaldehyde emission is similar to that reported for gasoline engines that the aromatic emissions are considerably smaller. For comparison, molar emission ratios reported by Cocker et al. [28] for a slowly moving ("creeping") diesel vehicle are included in Table 2. The emission ratios determined here are all considerably higher than that of Cocker et al. [28] although it should be noted that the emission ratios for the aromatic components are essentially at or below our detection limit. The acetaldehyde emissions are quite variable across the entire plume event and serve to illustrate the variable nature of the emissions of in-use vehicles.

3.4. Distribution of benzene and toluene—implications to photochemical air age determination

Another important implication of the current study is the difference in the distribution of benzene and toluene found in vehicle exhaust with that measured in the ambient air within the MCMA. This is because the ratio of these compounds is often used as an indicator of the photochemical age of an air mass. The benzene to toluene ratio can be used to deduce the photochemical age of an air mass based of the OH reactivity differences for the two compounds, but requires an accurate knowledge of the starting distribution of these two components [38]. While the ratio of these two compounds in an urban environment, like the MCMA, might be expected to be controlled predominately by vehicular emissions our data suggests that there are other contributing emission sources that influence the ratio of these compounds. This assertion is based on an analysis of all of the valid mobile data in this study, which indicates that the fleet averaged volumetric benzene to toluene ratio is 0.48 [8] while a significantly lower ratio of 0.23 is derived from both PTR-MS and GC-FID fixed site urban data contained in Fig. 3. These results indicate that the benzene to toluene ratio is higher in vehicle exhaust (examined from a fleet perspective and not an individual vehicle basis) than that observed in the ambient urban air. This result seems counterintuitive, since the OH radical reacts more rapidly with toluene than benzene [39], because photochemical processing of vehicle exhaust only serves to further increase the observed benzene to toluene ratio. The fleet averaged volumetric benzene to toluene ratio deduced from the results of the

experiments described in this study are found to be consistent with benzene to toluene ratios derived from other vehicle exhaust emission studies. The relative amounts of benzene and toluene measured in the exhaust from gasoline vehicles will be dependent on the overall efficiency of the emission control system, as catalytic converters are more efficient at removing toluene than benzene from the exhaust [23,32,33,35] and the MCMA vehicle fleet will be characterized by some distribution of vehicles with and without functioning emission control systems. The reported volumetric benzene to toluene ratios range from 0.24 [23] to 0.35 [32] for vehicles operated without catalytic converters and from 0.66 [23] to 1.31 [32] for vehicles possessing operational catalytic converters. Our present value falls between the no emission control and emission control ranges and is comparable to that measured in two Mexico City tunnels (0.42 and 0.35) in 1998 by Mugica et al. [27]. Our roadway measurements of benzene and toluene thus seem totally consistent with the results of vehicle tail pipe emission studies [23,32,33,35] as well as the results of a Mexico City tunnel study [27]. Our data suggests that vehicle emissions alone do not define the distribution of benzene and toluene in the MCMA urban environment. Large toluene solvent plumes were routinely encountered during our many drives within the MCMA and these non-vehicular emission sources of toluene appear to have a significant impact on the overall observed distribution of benzene and toluene in this urban airshed.

It is noted that similar conclusions may be drawn from measurements made in the US. The average urban US ambient air measurements indicate a volumetric benzene to toluene ratio of 0.44 [40]. These results are higher than that observed in the MCMA and probably reflect a higher percentage of emission controlled vehicles in the US than in Mexico City. Tunnel studies conducted in the US report volumetric benzene to toluene ratios of 0.61 and 0.78 [41]. These tunnel measurements should reflect vehicle fleet averaged emissions and again suggests that a greater proportion of benzene relative to toluene is present in vehicle emissions than in urban ambient air. Additional evidence is offered by two other PTR-MS studies of ambient urban air masses, one in The Netherlands [42] (0.27) and another off the US coast of New England [43] (0.27), which provide benzene to toluene ratios that are smaller than what would be anticipated from any fleet averaged vehicle exhaust profiles from either the US or Europe.

4. Conclusion

The PTR-MS has been shown to be an effective and efficient technique for quantifying selected exhaust emission products from in-use on-road vehicles. Mixing ratios deduced by the PTR-MS technique for benzene and toluene were found to correlate very well with GC-FID data from collocated canister samples. Other PTR-MS ion masses represent collections of compounds such as mass 57, 107 and 121. In this study it was found that mixing ratio deduced from the ion intensity at mass 57 agreed very well with the sum of the MTBE and isomeric butene concentrations derived from GC-FID measurements. The comparison of the PTR-MS mixing ratios deduced from the ion intensities at mass 107 and 121 showed significant deviations with the comparable C2 and C3-benzene measurements by GC-FID. While direct comparative data between the PTR-MS and another independent method is not available for the oxygenated species, evidence is provided that supports the reliable measurement of methanol, acetaldehyde and acetone by PTR-MS. Thus, this study serves to validate the PTR-MS technique as a quantitative monitor of selected components present in both vehicle tail pipe emissions and in the ambient air within heavily polluted environments like Mexico City.

Reliable high time response measurements like that collected using the mobile PTR-MS provides information not only into the emissions of individual vehicles but also allows assessment of fleet emission averages and distributions [5,8,44]. These measurements capture the wide range of vehicle emission variability caused by vehicle condition, fuel quality, driving behavior and other parameters that effect engine emissions. Emission variability is reflected in the frequency distribution of the on-road emission measurements. Statistical information derived from these frequency distributions can then be used to assess and validate emission inventories [8]. Vehicle emissions measured using the PTR-MS technique have been used to estimate fleet averaged emissions, which indicate that light duty vehicles in the MCMA have significantly higher VOC emissions than those found in US cities [5,8,44].

We noted that the distribution of benzene and toluene in vehicle exhaust (street level air) appears to be higher than the ratio observed in the ambient atmosphere at the fixed urban sampling sites. This counterintuitive result raises the question as to whether this observation is an experimental error or actually reflects real differences in these air masses. Our vehicle exhaust results were shown to be consistent with that of other vehicle exhaust emission studies, while our fixed site urban measurements were corroborated by GC-FID measurements so we do not attribute the variation in the benzene toluene ratios to experimental error. While additional study is required before any conclusive statements can be made, the results of this study suggest that there are other significant non-vehicle emission sources of toluene which influence the distribution of benzene and toluene in the urban MCMA environment.

Acknowledgements

Funding for the purchase of the PTR-MS instrument was through the National Science Foundation Major Research Instrumentation Program, Murdock Charitable Trust and Montana State University. Project funding was provided by funds from the Mexican Metropolitan Environmental Commission to the Integrated Program on Urban, Regional and Global Air Pollution at MIT and the National Science Foundation.

References

[1] L.T. Molina, M.J. Molina (Eds.), Air Quality in the Mexico Megacity: An Integrated Assessment, Kluwer Academic, Dordrecht, 2002, p. 21.
[2] R. Gakenheimer, L.T. Molina, J. Sussman, C. Zegras, A. Howitt, J. Markler, R. Lacy, R. Slott, A. Villegas, in: L.T. Molina, M.J. Molina

(Eds.), Air Quality in the Mexico Megacity: An Integrated Assessment, Kluwer Academic, Dordrecht, 2002, p. 213.
[3] L.T. Molina, M.J. Molina (Eds.), Air Quality in the Mexico Megacity: An Integrated Assessment, Kluwer Academic, Dordrecht, 2002, p. 1.
[4] S.C. Herndon, J.T. Jayne, M.S. Zahniser, D.R. Worsnop, B. Knighton, E. Allwine, B.K. Lamb, M. Zavala, D.D. Nelson, J.B. McManus, J.H. Shorter, M.R. Canagaratna, T.B. Onasch, C.E. Kolb, Faraday Discuss. 130 (2005) 327.
[5] C.E. Kolb, S.C. Herndon, B. McManus, J.H. Shorter, M.S. Zahniser, D.D. Nelson, J.T. Jayne, M.R. Canagaratna, D.R. Worsnop, Environ. Sci. Technol. 38 (2004) 5694.
[6] W. Lindinger, A. Hansel, A. Jordan, Int. J. Mass Spectrom. 173 (1998) 191.
[7] E.P. Hunter, S.G. Lias, NIST Chemistry Webbook. http://webbook.nist.gov/.
[8] M. Zavala, S.C. Herndon, R.S. Slott, E.J. Dunlea, L.C. Marr, J.H. Shorter, M. Zahniser, W.B. Knighton, T.M. Rogers, C.E. Kolb, L.T. Molina, M.J. Molina, Atmos. Chem. Phys. (2006) Submitted for publication.
[9] S.C. Herndon, J.H. Shorter, M.S. Zahniser, J. Wormhoudt, D.D. Nelson, K.L. Demerjian, C.E. Kolb, Environ. Sci. Technol. 39 (2005) 7984.
[10] J.H. Shorter, S. Herndon, M.S. Zahniser, D.D. Nelson, J. Wormhoudt, K.L. Demerjian, C.E. Kolb, Environ. Sci. Technol. 39 (2005) 7991.
[11] S.C. Herndon, T. Rogers, E.J. Dunlea, J.T. Jayne, R. Miake-Lye, W.B. Knighton, Environ. Sci. Technol. (2006) in press.
[12] C. Kolb, B. Lamb, B. Knighton, S. Herndon, E. Velasco, M. Zavala, Integrated Program on Urban, Regional and Global Air Pollution Newsletter, vol. 4, Fall 2003 (2003).
[13] AGU Fall Meeting 2004 San Francsico, California Megacity Impact on Air Quality I Posters A11A-0004.
[14] M. McFarland, D.L. Albritton, F.C. Fehsenfeld, E.E. Ferguson, A.L. Schmeltekopf, J. Chem. Phys. 59 (1973) 6620.
[15] T. Su, W.J. Chesnavich, J. Chem. Phys. 76 (1982) 5183.
[16] J. Zhao, R.Y. Zhang, Atmos. Environ. 38 (2004) 2177.
[17] J.A. de Gouw, C. Warneke, T. Karl, G. Eerdekens, C. van der Veen, R. Fall, Int. J. Mass Spectrom. 223 (2003) 365.
[18] T.J. Christian, B. Kleiss, R.J. Yokelson, R. Holzinger, P.J. Crutzen, W.M. Hao, T. Shirai, D.R. Blake, J. Geophys. Res. 109 (2004).
[19] J.A. de Gouw, P.D. Goldan, C. Warneke, W.C. Kuster, J.M. Roberts, M. Marchewka, S.B. Bertman, A.A.P. Pszenny, W.C. Keene, J. Geophys. Res. 108 (2003).
[20] M.J. Northway, J.A. de Gouw, D.W. Fahey, R.S. Gao, C. Warneke, J.M. Roberts, F. Flocke, Atmos. Environ. 38 (2004) 6017.
[21] W.C. Kuster, B.T. Jobson, T. Karl, D. Riemer, E. Apel, P.D. Goldan, F.C. Fehsenfeld, Environ. Sci. Technol. 38 (2004) 221.
[22] I. Schifter, L. Diaz, E. Lopez-Salinas, F. Ramos, S. Avalos, G. Lopez-Vidal, M. Castillo, Environ. Sci. Technol. 34 (2000) 3606.
[23] J.J. Schauer, M.J. Kleeman, G.R. Cass, B.R.T. Simoneit, Environ. Sci. Technol. 36 (2002) 1169.
[24] A.M. Diskin, T.S. Wang, D. Smith, P. Spanel, Int. J. Mass Spectrom. 218 (2002) 87.
[25] B.T. Jobson, M.L. Alexander, G.D. Maupin, G.G. Muntean, Int. J. Mass Spectrom. 245 (2005) 78.
[26] C. Warneke, J.A. de Gouw, W.C. Kuster, P.D. Goldan, R. Fall, Environ. Sci. Technol. 37 (2003) 2494.
[27] V. Mugica, J. Watson, E. Vega, E. Reyes, M.E. Ruiz, J. Chow, Sci. World J. 2 (2002) 844.
[28] D.R. Cocker, S.D. Shah, K.C. Johnson, X.N. Zhu, J.W. Miller, J.M. Norbeck, Environ. Sci. Technol. 38 (2004) 6809.
[29] J.J. Schauer, M.J. Kleeman, G.R. Cass, B.R.T. Simoneit, Environ. Sci. Technol. 33 (1999) 1578.
[30] W.O. Siegl, R.H. Hammerle, H.M. Herrmann, B.W. Wenclawiak, B. Luers-Jongen, Atmos. Environ. 33 (1999) 797.
[31] D. Smith, P. Cheng, P. Spanel, Rapid Commun. Mass Spectrom. 16 (2002) 1124.
[32] N.V. Heeb, A.M. Forss, C. Bach, S. Reimann, A. Herzog, H.W. Jackle, Atmos. Environ. 34 (2000) 3103.
[33] N.V. Heeb, A.M. Forss, C. Bach, P. Mattrel, Atmos. Environ. 34 (2000) 1123.
[34] C. Warneke, J.A. de Gouw, E.R. Lovejoy, P.C. Murphy, W.C. Kuster, R. Fall, J. Am. Soc. Mass Spectrom. 16 (2005) 1316.
[35] N.V. Heeb, A.M. Forss, C. Bach, Atmos. Environ. 33 (1999) 205.
[36] M.R. Canagaratna, J.T. Jayne, D.A. Ghertner, S. Herndon, Q. Shi, J.L. Jimenez, P.J. Silva, P. Williams, T. Lanni, F. Drewnick, K.L. Demerjian, C.E. Kolb, D.R. Worsnop, Aerosol Sci. Technol. 38 (2004) 555.
[37] R.A. Harley, L.C. Marr, J.K. Lehner, S.N. Giddings, Environ. Sci. Technol. 39 (2005) 5356.
[38] J.M. Roberts, F.C. Fehsenfeld, S.C. Liu, M.J. Bollinger, C. Hahn, D.L. Albritton, R.E. Sievers, Atmos. Environ. 18 (1984) 2421.
[39] R. Atkinson, J. Arey, Chem. Rev. 103 (2003) 4605.
[40] D.D. Parrish, M. Trainer, V. Young, P.D. Goldan, W.C. Kuster, B.T. Jobson, F.C. Fehsenfeld, W.A. Lonneman, R.D. Zika, C.T. Farmer, D.D. Riemer, M.O. Rodgers, J. Geophys. Res. 103 (1998) 22339.
[41] J.C. Sagebiel, B. Zielinska, W.R. Pierson, A.W. Gertler, Atmos. Environ. 30 (1996) 2287.
[42] C. Warneke, C. van der Veen, S. Luxembourg, J.A. de Gouw, A. Kok, Int. J. Mass Spectrom. 207 (2001) 167.
[43] J.A. de Gouw, A.M. Middlebrook, C. Warneke, P.D. Goldan, W.C. Kuster, J.M. Roberts, F.C. Fehsenfeld, D.R. Worsnop, M.R. Canagaratna, A.A.P. Pszenny, W.C. Keene, M. Marchewka, S.B. Bertman, T.S. Bates, J. Geophys. Res. 110 (2005).
[44] M. Jiang, L.C. Marr, E.J. Dunlea, S.C. Herndon, J.T. Jayne, C.E. Kolb, W.B. Knighton, T.M. Rogers, M. Zavala, L.T. Molina, M.J. Molina, Atmos. Chem. Phys. 5 (2005) 3377.